AIAA JOURNAL
Vol. 44, No. 11, November 2006

Scaling of Fully Pulsed Jets in Crossflow

Hamid Johari*
Worcester Polytechnic Institute, Worcester, Massachusetts 01609

DOI: 10.2514/1.18929

There is recent interest in the dynamics of pulsed jets in uniform crossflow. A classification scheme for fully pulsed jets in crossflow is proposed based on the stroke ratio of the jet pulse and the duty cycle of the pulse train. Scaling relations for penetration and dilution of fully pulsed jets in crossflow are derived from the self-similar scaling of turbulent vortex rings and puffs in quiescent media. Individual turbulent structures are assumed to drift freely with the crossflow in the proposed scaling. The penetration of fully pulsed jets scales with the fourth root of the velocity ratio, stroke ratio, and axial distance. The decay of mean concentration scales with the velocity ratio and axial distance to the −3/4th power. These scaling relations apply to distinct turbulent structures before any interaction between successive structures. The criteria for interaction among flow structures near the nozzle and in the far field are also presented.

I. Introduction

THE steady jet in uniform crossflow (transverse jet) is a canonical three-dimensional flowfield that has been investigated extensively by analytical, experimental, and numerical approaches in the past 50 years. This flow is not only interesting from a fundamental perspective, but also has important practical applications in combustion and propulsion. The steady jet in crossflow has a complicated structure, and the details of velocity and passive scalar field have only been clarified in the past few years. Margason [1] has carried out a review of the steady transverse jet.

Before considering how pulsations modify the penetration and mixing of transverse jets, the characteristics of steady transverse jets are summarized briefly. Two separate regions can be identified in the transverse jet, namely: the near field (including the potential core and the transition zone) and the far field. These regions are shown schematically in Fig. 1. The potential core is characterized by a nearly uniform velocity and concentration region. In the transition zone the jet deflects more substantially, and in the normal (y–z) plane deforms (in the mean) into a kidney-shaped form. Based on velocity measurements, Fearn and Weston [2] attributed the kidney-shaped profile to a pair of counter-rotating, streamwise vortices. This counter-rotating vortex pair plays an important role in the far field of the jet [3]. Other vortical structures associated with transverse jets are discussed by Fric and Roshko [4]. Recent findings of Mungal and coworkers [5,6] have provided the scaling for the near and far fields of the steady jet in crossflow.

The jet trajectory and passive scalar mixing rate are of primary interest in steady transverse jet studies. The jet trajectory is typically correlated by the following expression:

$$\frac{y}{rd} = A\left(\frac{x}{rd}\right)^m \tag{1}$$

where d is the nozzle diameter and r is the jet-to-crossflow velocity ratio, $r = U_j/U_\infty$. Depending on the definition of jet trajectory and whether the velocity or passive scalar field is considered, A and m take on different values. If the locus of maximum concentration is used as the jet centerline, then m is in the range of 0.25–0.28, with A between 1.5–2.05 [5,7,8]. The jet trajectory based on the velocity field results in m values close to the theoretically predicted value of one-third [3,6]. The jet concentration decays as $(s/rd)^{-1.3}$ in the near field and as $(s/rd)^{-2/3}$ in the far field; s is the arclength along the jet trajectory [5]. The transition from the near field to the far field has been correlated with $x \sim 0.2r^2d$ [5]. Keffer and Baines [9] showed the utility of the r^2d scaling in their near field study. The penetration of heated, steady transverse jets has been characterized in terms of the momentum-flux ratio $(\rho_j/\rho_\infty)\ r^2$ by Kamotani and Greber [10]. Karagozian [11] analytically examined dynamics of the streamwise vortex pair and its implications for the jet penetration. A recent numerical study [12] has showed that besides r, the nozzle velocity profile and the oncoming boundary layer thickness affect the penetration of steady jets in crossflow.

Unsteadiness at the jet source impacts the evolution of free jets in quiescent media. Crow and Champagne [13] observed that small periodic forcing at the jet exit produces a large increase in the near field spreading rate. Vermeulen et al. [14] studied the effects of high amplitude acoustic pulsing of the jet and observed an increase in entrainment up to a certain downstream location from the jet exit. Bremhorst and Hollis [15] found that the entrainment rate of fully modulated free jets (where the jet flow was completely shut off during part of the cycle) was approximately twice that of the steady jet with the same mean velocity. Recently, Krueger and Gharib [16] examined the augmentation of thrust afforded by fully pulsed jets. As much as 90% thrust augmentation was measured for specific forcing conditions.

Kelso et al. [17] forced a jet in crossflow, at a frequency close to that of the shear layer surrounding the jet, with an amplitude equal to 10% of the jet exit velocity. They observed an increase in the size of vortex rings found in the jet near field. In an acoustically pulsed transverse jet, Vermeulen et al. [18] found a significant increase in jet spread and a penetration increase of up to 92%. The study of Wu et al. [19] showed that at low pulsing frequencies a jet in crossflow can penetrate up to 4 times deeper than a steady jet for the same mean momentum flux.

Fully modulating the jet can drastically modify the flowfield and significantly increase the jet penetration compared to the steady jet. Figure 2 compares the penetration and structure of a fully pulsed jet with a steady jet at low Reynolds number (650) in the experiments of Eroglu and Breidenthal [20]. The pulsed jet consists of a sequence of vortex rings that penetrate deeply into the crossflow in comparison with the steady jet. In this set of experiments, the duty cycle (the fraction of jet-on during each cycle) was $\alpha = 0.5$, and the stroke ratio associated with each pulse is estimated to be $\approx$1.8. Experiments at higher Reynolds number (6200) shown in Fig. 3 also reveal a series of turbulent vortex rings, which penetrate deeper (up to 100%) into the crossflow than the steady jet [20]. The stroke ratio in Fig. 3 is estimated to be $\approx$13 with $\alpha = 0.5$. Interestingly, the vortex rings are followed by a stream of jet fluid that has a trajectory nearly the same

Presented as Paper 0304 at the 43rd AIAA Aerospace Sciences Meeting and Exhibit, Reno, NV, 10–13 January 2005; received 18 July 2005; revision received 31 January 2006; accepted for publication 4 July 2006.

*Professor, Mechanical Engineering Department, 100 Institute Road. Associate Fellow AIAA.

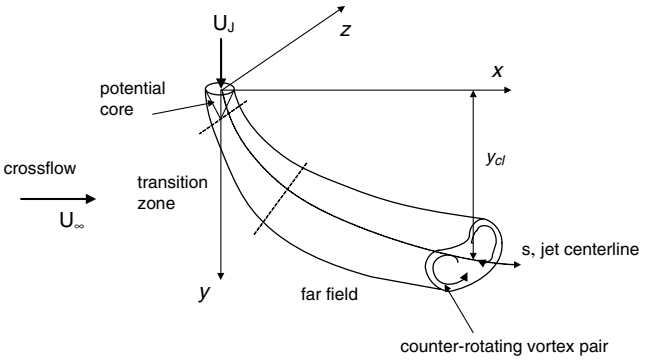

Fig. 1 Schematic sketch of a steady jet in crossflow.

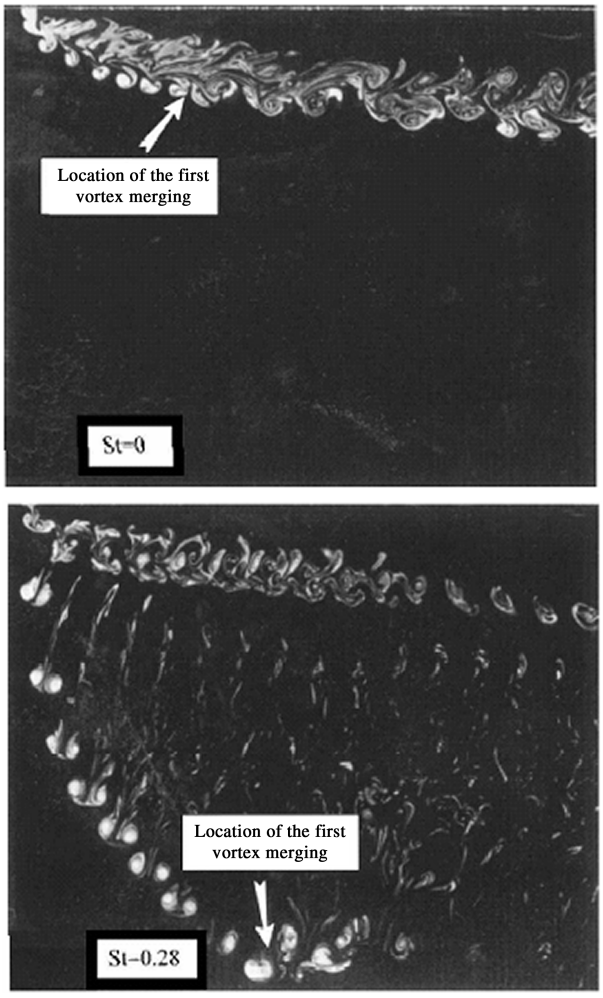

Fig. 2 Comparison of steady a) and fully pulsed b) jets at a low Reynolds number of 650. The pulsed jet has a duty cycle of 0.5, and the stroke ratio is 1.8. Locations of first interactions among the laminar vortex rings are indicated by the arrows. Images are from [20], reprinted by permission of the American Institute of Aeronautics and Astronautics, Inc.

as the steady jet. The jet is composed of two streams, one penetrating deeply into the crossflow and consisting of vortex rings and the other following the steady jet trajectory. Chang and Vakili [21] similarly observed that an individual vortex ring can penetrate deeply into the crossflow due to the self-induced velocity of the ring. The dilution and mixing of strongly pulsed jets in crossflow have been studied in [8,20]. The overall mixing rate, as indicated by the "flame" length, of the pulsed jets in [20] was increased by 50% at an optimum pulsing condition.

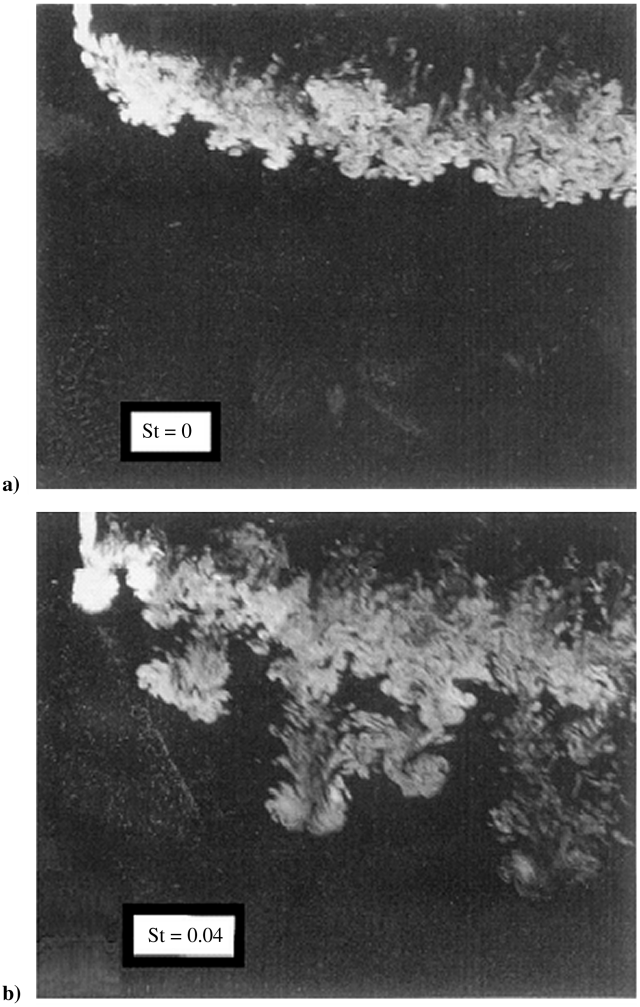

Fig. 3 Comparison of steady a) and fully pulsed b) jets at a Reynolds number of 6200. The pulsed jet has a duty cycle of 0.5, and the stroke ratio is 13. Images are from [20], reprinted by permission of the American Institute of Aeronautics and Astronautics, Inc.

The effects of duty cycle on the penetration of jets in crossflow were examined in aqueous media by Johari et al. [8]. Two fully pulsed jets with nearly the same stroke ratio, and duty cycles of 0.3 and 0.5, are compared with a steady jet of the same velocity in Fig. 4. For the lower duty cycle jet, the flowfield consists of well-separated, individual vortical structures that stem from the jet starting vortex ring. These structures penetrate into the crossflow more than the steady jet. The structures in the higher duty cycle jet penetrate somewhat less than the lower duty cycle case; however, there are substantial interactions among successive pulses in the former case. With increasing duty cycle, distance between the consecutive vortical structures decreases resulting in increased interaction and reduced penetration.

In the majority of past work on pulsed jets in crossflow, either sinusoidal forcing has been pursued or the duty cycle for fully modulated pulsing has been fixed at $\alpha = 0.5$. McCloskey et al. [22] have examined square wave pulsing of air jets, with duty cycles in the range of $\sim$0.2–0.6. Strongly pulsed jets at low duty cycles ($\sim$0.2–0.3) create compact vortex rings that penetrate deeply into the crossflow. As the duty cycle increases, successive vortex rings get closer together and eventually interact, resulting in the destruction of ring structure. Enhanced penetration has also been observed recently with zero-net-mass-flux (synthetic) jets in crossflow, where the near field is dominated by individual vortex rings [23].

In this paper we examine the trajectory of fully modulated jets by using the self-similar scaling of turbulent vortex rings and puffs [24] (mass of turbulent fluid with distributed vorticity) in quiescent media. The interplay between the pulse temporal width (injection

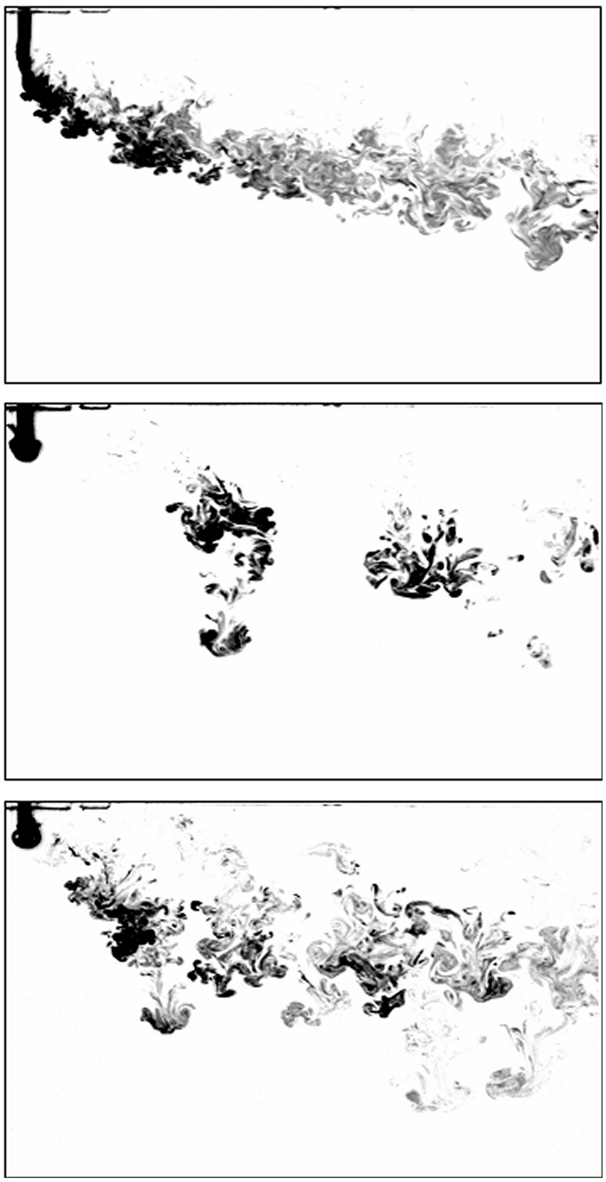

Fig. 4 Steady and fully pulsed jets in crossflow at a velocity ratio of 5: a) steady; b) duty cycle 0.3; and c) duty cycle 0.5. Stroke ratio is the same for the pulsed jets. The starting vortex ring near the nozzle and the vortical structures further downstream are clearly visible. These contrast-enhanced images are from [8].

time) and the pulsing duty cycle is specifically addressed in conjunction with the jet trajectory.

II. Pulsed Jet Structure

We propose that strongly pulsed jets, where the root-mean-square velocity is substantially greater than the time averaged velocity at the nozzle and the slug of jet fluid associated with each pulse is relatively short, generate a series of compact vortex rings or puffs that penetrate greatly into the crossflow. The variety of flow features and trajectories found in pulsed crossflow jets is a result of the different flow structures formed during the pulse initiation and the subsequent interaction between them. Here, we define a jet-to-crossflow velocity ratio based on the average jet velocity *during the pulse*, $r_p = \bar{U}_j/U_\infty$. Thus, we can compare a pulsed jet with a steady one having the same velocity ratio during the pulse and independent of the mean jet velocity. Henceforth, we will focus on pulsed jets with velocity ratio, during the injection, greater than $r_p \geq 3$, and nozzle diameters much greater than the oncoming boundary layer thickness.

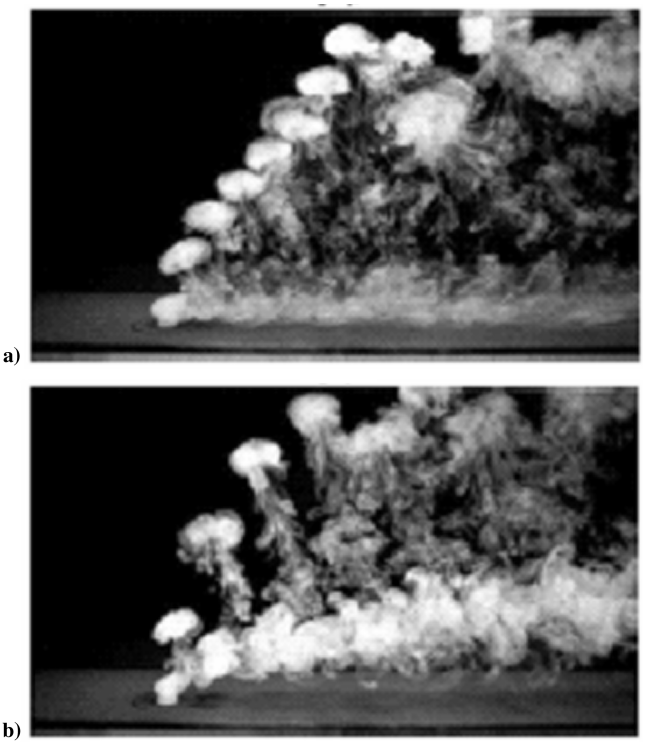

Fig. 5 Pulsed jets: a) $\alpha = 0.31$ and $L/d \approx 3.8$, and b) $\alpha = 0.15$ and $L/d \approx 7.5$. Images are from [22], reprinted by permission of Cambridge University Press.

In this manner, weak jets and cases with appreciable upstream boundary layer influence are excluded.

The leading vortex ring of a starting freejet has been shown to separate from the rest of the jet column [25,26]. Moreover, the formation of the leading vortex is associated with the first slug of fluid ejected from a nozzle (or orifice) having a length of $\sim 4d$ [26]. The stoke length L for a pulse of (temporal) width τ through a nozzle of area A is defined by

$$L = \frac{1}{A}\int_0^\tau \int_A u_j \, \mathrm{d}A \, \mathrm{d}t = \bar{U}_j \tau \tag{2}$$

where u_j is the jet velocity at the nozzle exit. Then, pulsed free jets having a stroke ratio of $L/d > 4$, create leading vortex rings followed by a trailing jet column [16]. For $L/d < 4$, only individual vortex rings get formed and the ring circulation and impulse are dependent on the slug length and exit velocity. The images in Fig. 5, from the work of Karagozian and coworkers [22], show pulsed jets in crossflow with stroke ratios of approximately 3.8 and 7.5, and duty cycles of 0.31 and 0.15, respectively. The close proximity of the vortex rings in the case with the larger duty cycle is notable. The maximum penetration is nearly the same in the two cases. However, the trailing jet fluid following the vortex rings in the lower stream (closer to the wall) is clearly evident only in the larger stroke ratio case. A stream close to the wall is also visible in Fig. 3b.

If the pulsed jet emerges from a nozzle or a sharp orifice where the vorticity is confined to the jet perimeter, then compact core vortex rings are created. The jets in Figs. 2, 3, and 5 exited through a nozzle and resulted in compact vortex rings. Alternatively, jets emerging from a long pipe where the vorticity is spread across the jet width produce turbulent puffs, with the vorticity distributed in a spherical volume larger than that of compact vortex rings. Turbulent puffs are also created when the slug lengths much larger than that associated with the vortex ring formation are associated with a pulsed jet. The nozzle velocity profile affecting the formation of individual vortical structures in pulsed jets is analogous to the effect that the nozzle velocity profile has on the penetration of steady jets; see [12].

Considering the physics of pulsed and starting freejets, the jet fluid slug length ejected during each pulse and the spatial separation

between successive flow structures are the two fundamental parameters governing the dynamics of strongly pulsed jets in crossflow. In essence, the slug length (and the pulse width τ) controls the initial flow structure, with smaller values leading to compact vortex rings and larger values to puff-like structures. On the other hand, the spatial separation (and the duty cycle α) sets the degree of interaction among the successive flow structures. For a fixed jet velocity and nozzle diameter, pulse width τ and duty cycle α are the parameters that control the jet structure and trajectory. Of course, the pulse velocity ratio does play a role; however, it becomes a critical parameter for weak jets with low r_p. In addition, the relevant velocity in pulsed jets is that during the pulse, and not the time averaged value, since the former is responsible for the formation of flow structures. Controlling the duty cycle as an independent parameter allows the separate specification of the pulse width τ and frequency f, with implications for the jet structures and the nature of their interaction. The duty cycle is related to these two parameters through $\alpha = f\tau$.

For strongly pulsed jets at small duty cycles, that is, with sufficient spatial separation to create isolated structures near the nozzle, the jets may consist of individual vortex rings, vortex rings followed by a fluid column, turbulent puffs, or a segment of steady jet, depending on the slug length ejected with each pulse. For slug lengths less than about $4d$, individual vortex rings are created. The value of the stroke ratio segregating the creation of an individual vortex ring and vortex rings followed by a fluid column is based on the freejet studies and the images of pulsed jets in [20,22,27]. This value is directly correlated with vorticity flux of the rolled-up vortex sheet during the ring formation and is dependent on whether a nozzle or straight pipe is used [28], and possibly the approaching boundary layer [12]. For large velocity ratios, the critical stroke ratio should asymptotically approach the value of 4 associated with freejets with a top-hat profile.

As the stroke ratio increases beyond the threshold value of $\sim 4d$, the pulsed jet will bifurcate into two streams, one corresponding to the deep penetration of vortex rings and the other associated with the trailing jet fluid. The latter is expected to have a trajectory close to that of the steady jet in crossflow. The two-branch pulsed jets have been reported by Gordon et al. [23] and are visible in the images of [8,20,22]. The relative amount of fluid transported by the vortex rings, compared to the rest of the jet, decreases as the stroke ratio increases. Eventually the amount of jet fluid trailing the vortex ring becomes much greater than that in the vortex ring, and the jet consists of a series of puffs in crossflow. Based on the available data, this transition is thought to occur at a stroke ratio of $L/d \sim 20$–23. For the zero-net-mass-flux jet in crossflow, a critical stroke ratio of ~ 23 has been reported [23]. The penetration of puffs will be less than that of vortex rings due to the distributed vorticity and greater entrainment rate of puffs.

As the stroke length increases even further, the flow asymptotes to a starting jet in crossflow. The penetration of the latter is expected to be comparable to that of a steady jet, and the flow appears as an interrupted steady jet in crossflow; see Fig. 6 in [8]. The last transition is thought to occur at a stroke ratio of $L/d \sim 75$. The various flow regimes for strongly pulsed jets in crossflow at small duty cycles are summarized later on.

It should be pointed out that the stated values for the threshold stroke ratios are based on the limited available data, and more importantly, they may be somewhat configuration dependent. More data are needed to elucidate these transition boundaries and verify the regimes proposed.

III. Interaction Among Structures

The flow features discussed in the previous section will be present only when they exist in isolation. Any interaction with a neighboring flow structure will alter the vorticity distribution within the structure and may modify the flow to a quasisteady jetlike state. The spatial separation of structures near the nozzle can be approximated by the celerity of structure multiplied by the temporal separation between successive pulses. The latter is a function of the duty cycle and is equal to $(1-\alpha)\tau/\alpha$. The celerity near the nozzle is due to the freestream and vortical structure convective velocities or approximately $\sqrt{U_\infty^2 + (\bar{U}_j/2)^2} = U_\infty\sqrt{1 + r_p^2/4}$. The spatial separation should be compared with the length scale of the structure. For the case of vortex rings, a ring will be affected if it is within $\sim 2d$ of its neighbors. Thus, interaction among flow structures will be expected in the vicinity of the nozzle if

$$\frac{1-\alpha}{\alpha}\tau U_\infty\sqrt{1 + r_p^2/4} < 2d \tag{3}$$

For the case of large velocity ratio jets, the above expression simplifies to $L/d < 4\alpha/(1-\alpha)$.

A map for the various flow regimes is presented in Fig. 6. The right-hand region indicates the combination of duty cycle and stroke ratios where the flow structures are expected to be interacting in the near field. The left hand shows the region where distinct flow structures are expected. The various flow structures listed in Table 1 are delineated in this region. Experimental data from several references are also plotted in Fig. 6 to support the proposed classification.

Table 1 Various pulsed jets in crossflow structures

Stroke ratio	Flow structure
$L/d \lessapprox 4$	Compact vortex rings
$\sim 4 < L/d \lessapprox 20$	Vortex rings/puffs + trailing column
$\sim 20 < L/d \lessapprox 75$	Turbulent puffs
$L/d \gtrapprox 75$	Interrupted steady jet segments

Even though the flow structures may be isolated in the near field, they will interact at some point along their trajectory. The reason is that the spatial separation among successive structures gets reduced as they move downstream. The passage time of a flow structure is given by $\sim \delta/(\mathrm{d}s/\mathrm{d}t)$, where δ is a length scale of the structure and $\mathrm{d}s/\mathrm{d}t$ is its celerity along the jet trajectory. The passage time increases continuously due to the decreasing celerity and increasing δ. At a certain point along the trajectory, the passage time becomes comparable to the pulsing period τ/α. Thereafter, the flow structures will interact and their initial characteristics will change to a quasisteady jetlike state. The approximate point of interaction can be found by equating the pulsing period with the individual structure's passage time,

$$\frac{(\mathrm{d}s/\mathrm{d}t)\tau}{\alpha\delta(x)} \approx 1 \tag{4}$$

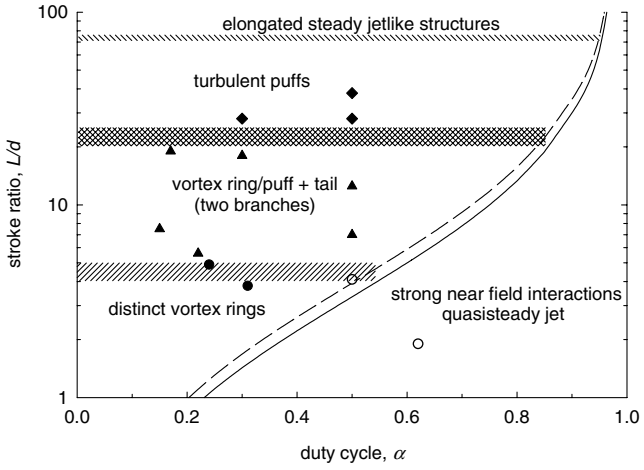

Fig. 6 Map for the various flow regimes of fully pulsed jets as a function of the stroke ratio and duty cycle. The experimental data from [8,20–22] refer to distinct vortex rings (●), vortical structures with trailing column (▲), turbulent puffs (◆), and interacting structures (○). The solid and dashed curves represent Eq. (3) for velocity ratios of 3 and 10, respectively.

Given τ and α, the celerity and growth rate, the location of the first interaction can be found from Eq. (4).

IV. Pulsed Jet Trajectory

The impulse I of incompressible turbulent vortex rings and puffs is conserved in quiescent media, away from the generator. In the self-similar region, Glezer and Coles [29] and Richards [24] express the motion of vortex rings and puff by the following expression:

$$y - y_o = k\left[\frac{I}{\rho}(t - t_o)\right]^{1/4} \tag{5}$$

where y_o and t_o are the virtual origin in space and time. These parameters are typically negative for thin-cored vortex rings and positive for puffs. The proportionality constant k has an experimentally determined value of ~25 for an individual turbulent vortex ring [29] and ~3 for a distinct puff in quiescent media [24,30,31]. In a study of individual puffs in crossflow, Diez et al. [31] have shown that a puff drifts in the crossflow direction with a velocity of U_∞, that is, $x = U_\infty(t - t_o)$. If we assume that the same holds for vortex rings, elimination of time in Eq. (5) will produce the trajectory for pulsed jets consisting of noninteracting vortex rings or puffs. The only difference between the rings and the puffs is expected to be the proportionality constant k.

In the self-similar region, the trajectory of pulsed jets consisting of noninteracting vortex rings or puffs will be

$$y - y_o = k\left(\frac{Ix}{\rho U_\infty}\right)^{1/4} \tag{6}$$

The expression in Eq. (6) ignores any bending or tilting of the vortex ring resulting from the presence of crossflow. The jet impulse at the nozzle can be computed as follows:

$$I = \int_0^\tau \int_A \rho u_j^2 \, \mathrm{d}A \, \mathrm{d}t = \rho \bar{U}_j^2 \frac{\pi}{4} d^2 \tau P \tag{7}$$

where P is a parameter to account for any nonuniformity of jet velocity during the pulse. For an ideal square-wave pulse, $P = 1$. All other jet velocity time histories have a larger P, but they are typically in the range of 1.05–1.5 [32].

Substituting for impulse in the trajectory expression of Eq. (6), the latter can be rewritten as

$$\frac{y - y_o}{d} = k\left(r_p \frac{L}{d}\right)^{1/4}\left(\frac{x}{d}\right)^{1/4} \tag{8}$$

The factor of $\pi P/4$ has been neglected in the above expression, and L refers to the slug length for each pulse, as defined in Eq. (2). In this form, the trajectory expression is similar to that of Eq. (1) for the steady jet. For distinct vortex rings and puffs, the trajectory scales with the stroke ratio raised to one-fourth power. For pulsed jets with stroke ratios from 5 to 20, a stroke ratio of 4 should be used in Eq. (8) because only the first $4d$ slug contributes to the peak penetration. When compared with a steady jet in crossflow, pulsed jets have a much weaker dependence on the velocity ratio, $r_p^{1/4}$ vs $r^{0.73}$. Moreover, the trajectory of pulsed jets scales with a power of x slightly less than that for the steady jet. Although Chang and Vakili [21] propose a length scale to correlate the penetration of fully pulsed jets, the parameters involved can only be measured from the experiments, and as such the proposed length scale is not useful for predictive purposes.

The penetration of steady and pulsed jets with distinct vortical structures at velocity ratios of 5 and 10 is plotted in Fig. 7. For the steady jet, Eq. (1) is used with values of 1.5 and 0.27 for A and m, respectively [5]. For the pulsed jets, Eq. (8) is employed with proportionality constant k values of 13 and 3 for compact vortex rings and puffs, respectively. The chosen value of k for pulsed jets consisting of compact vortex rings is about one-half of the value for an individual ring in quiescent media. The reason for this choice is a more reasonable correspondence with the available pulsed jet data.

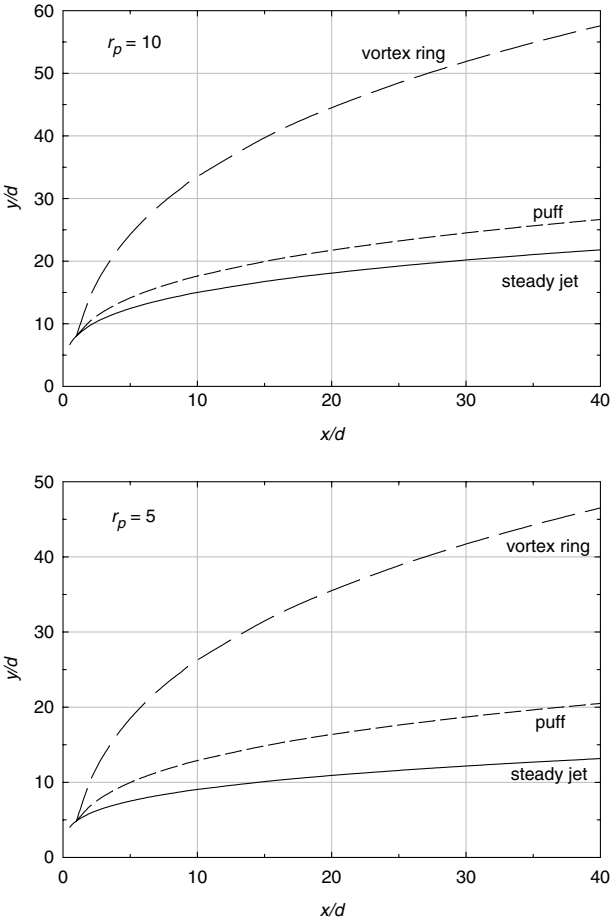

Fig. 7 Trajectory of steady and pulsed jets consisting of noninteracting vortex rings and puffs. Stroke ratios for the vortex rings and puffs are 4 and 28, respectively. Velocity ratios are 10 in a) and 5 in b).

To account for the virtual origin effects, the penetration of pulsed jets at $x = 1d$ was set equal to that of the steady jet. The pulsed jets consisting of distinct vortex rings in Fig. 7 have a stroke ratio of 4; those consisting of distinct puffs have a stroke ratio of 28. These conditions correspond approximately with specific cases in the experiments of McCloskey et al. [22] and Johari et al. [8], respectively. Clearly, the jet made of distinct vortex rings penetrates much further than the steady jet or the jet consisting of puffs. Because the penetration of pulsed jets is a weak function of the velocity ratio

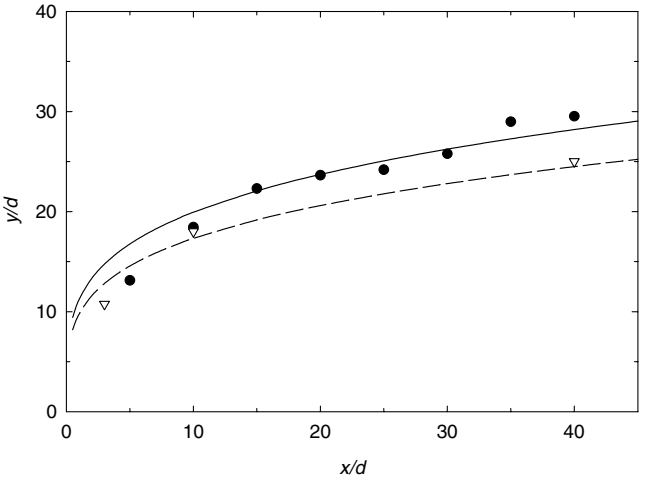

Fig. 8 Comparison of pulsed jet penetration for a duty cycle of 0.3 (●) from [8] with the model (solid line), and a duty cycle of 0.5 (▽) from [20] with the model (dashed line).

r_p, the pulsed jets' penetration relative to the steady jet is greater at the lower r_p. The predicted penetration for the jet consisting of vortex rings is the largest penetration expected because increasing the stroke length beyond 4 would only leave the extra jet fluid in a stream closer to the wall. Also, the penetration of a pulsed jet consisting of puffs would never reach the level associated with the vortex rings at any velocity ratio. These plots are in general agreement with the observations in [8,22].

To quantitatively compare the scaling laws for the trajectory of pulsed jets with the available data, the penetration of pulsed jets with a duty cycle of $\alpha = 0.3$ and $r_p = 4.2$ from [8] and those with a duty cycle of $\alpha = 0.5$ and $r_p = 8.8$ from [20] are plotted in Fig. 8. The data correspond to pulsed jets consisting of noninteracting vortical structures. A value of $k = 4$ was used in Eq. (8) to fit the two sets of data and virtual origin $y_o = 0$. The data from [8] correlate with the model very well after $15d$, with an average deviation of less than 3% and a maximum deviation of 6%. Similarly, the data from [20] correlate well with the model's prediction with deviations of 4% at $10d$ and 2% at $40d$. The largest deviation of 22% between the model and the data of [8] occurs in the near field at $x = 5d$; the discrepancy is caused by the fact that the trajectory expressions are valid only in the far field. It appears that, at least for these cases, the model in Eq. (8) is able to predict the penetration reasonably away from the jet source and before any interaction between successive structures.

From the trajectory expression in Eq. (8), the celerity of distinct vortex rings and puffs in the self-similar region can be found by $\mathrm{d}s/\mathrm{d}t = \sqrt{(\mathrm{d}y/\mathrm{d}t)^2 + U_\infty^2}$. Given the celerity and the growth rate of the flow structure, the point where the structures first start to interact can be estimated from Eq. (4) for various pulsing parameters. The data of Diez et al. [31] provide the dependence of puff width δ on y as follows:

$$\delta \approx 0.24(y - y_o) \tag{9}$$

Substituting the above expressions in Eq. (4), the point of interaction (x^*/d) of puffs in a pulsed jet can be found from the implicit expression

$$\frac{L/d}{0.28\alpha r_p k}[(r_p L/d)^{-1/2}(x^*/d)^{-1/2} + k^2(x^*/d)^{-2}]^{1/2} \approx 1 \tag{10}$$

The proportionality constant k in Eq. (10) is the same as that in Eq. (8) for puffs. For the case of vortex rings, the width δ can be assumed to be approximately constant.

The axial position of interaction for pulsed jets consisting of vortex rings and puffs is plotted in Fig. 9 as a function of duty cycle α. Stroke ratios of 4 and 28 were assumed in Fig. 9 for the vortex ring and puff cases, respectively. To account for the virtual origin effects, the duty cycle at which interactions are present in the near field was

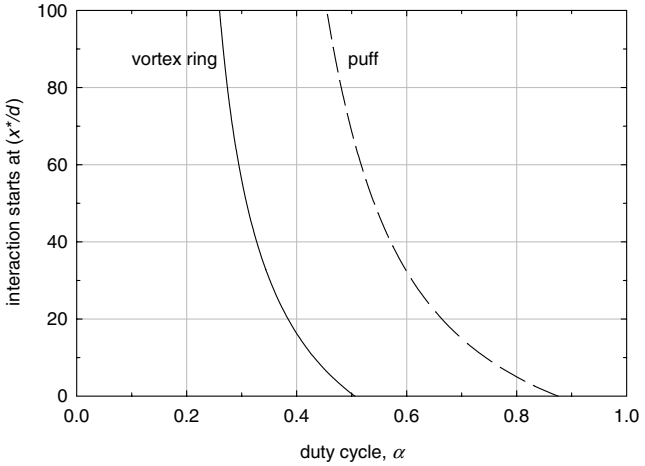

Fig. 9 Location where pulsed jet structures first interact. Stroke ratios are 4 for the vortex rings and 28 for the puffs. Velocity ratios for the jet consisting of vortex rings and puffs are 10 and 5, respectively.

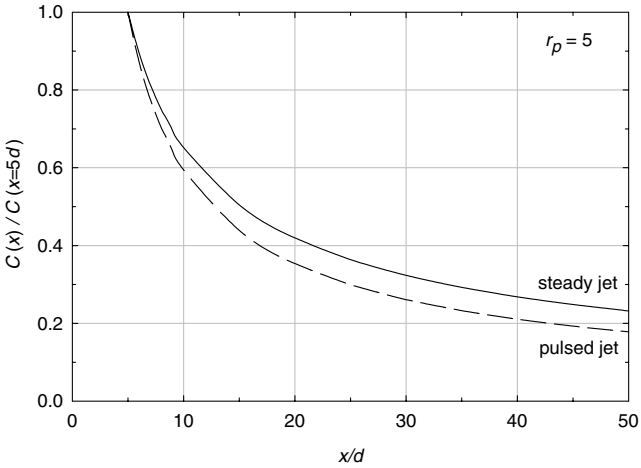

Fig. 10 Concentration, normalized by the value at $x = 5d$, of steady and pulsed jets consisting of distinct puffs for velocity ratio $r_p = 5$.

used. For the specific case of puffs considered here, a duty cycle of 0.87 causes interactions at the nozzle. Reducing the duty cycle to 0.45 moves the location of first interaction to $x^* = 100d$. On the other hand, distinct vortex rings are created at the nozzle for the range of duty cycles below 0.5. For $\alpha > 0.5$, vortex rings interact in the near field. The interaction is delayed to $x^* = 100d$ when the duty cycle is decreased to $\approx$0.26. Reducing the duty cycle further places the point of first interaction even further downstream. These predictions are qualitatively consistent with the images in [8,22], in that the reduction of duty cycle results in delay of interaction of successive structures. No quantitative data are available to allow a direct comparison with the predicted location of the first interaction.

V. Mixing

To assess the passive scalar mixing of pulsed jets in crossflow, the decay of concentration within individual puff structures is considered. Although the jet fluid in the cores of thin vortex rings remains relatively unmixed while the ring structure is maintained, the bubble of fluid surrounding the core gets mixed with the ambient fluid rapidly. The mixing of fluid in the bubble is expected to scale the same way as in a turbulent puff.

The puff volume V scales with the cube of diameter, $V \sim \delta^3$. The dependence of δ on y is provided in Eq. (9) for turbulent puffs in crossflow. Thus, the puff volume is expected to scale as

$$V \sim [(r_p L/d)^{1/4}(x/d)^{1/4}d]^3 \tag{11}$$

Volumetric arguments require that the decay of mean concentration C within a turbulent puff be directly proportional to $(V/V_o)^{-1}$, where $V_o = (\pi d^2 L)/4$ is the injected volume during each pulse. Thus, the mean concentration in a pulsed jet in crossflow consisting of individual puffs scales as

$$C(x) \sim r_p^{-3/4}(L/d)^{1/4}(x/d)^{-3/4} \tag{12}$$

This expression shows that the mean concentration decays as $(x/d)^{-3/4}$ for individual puffs in the self-similar region of fully pulsed jets.

For a steady jet in crossflow, the decay of centerline concentration is provided in [6] by

$$C_{\mathrm{cl}}/C_o = [(3/2A)r^{1/3}(x/d)^{2/3} + 1/2]^{-1} \tag{13}$$

where A is the same constant as in Eq. (1). The above expression reduces to the well-established $(x/d)^{-2/3}$ decay power law in the far field. Comparing the expression for the steady jet with Eq. (12) reveals that the mean concentration in pulsed jets decays somewhat more rapidly since the power of x is $-3/4$ as compared to $-2/3$. Moreover, there is a stronger dependence on the velocity ratio for pulsed jets than for the steady case. To compare the relative mixing of

pulsed and steady jets away from the nozzle vicinity, the mean concentration is normalized with the same at $x = 5d$ and plotted in Fig. 10 for $r_p = 5$. A pulsed jet consisting of distinct puffs gets 23% more diluted than a steady jet between 5 and $50d$. The relative decay of concentration in pulsed jets consisting of noninteracting puffs showed good correspondence with the limited dilution data in [8]. In the range of $x = 20$ to $50d$, the average deviation between the model and the data was 10%, with the largest deviation of 22% at $x = 20d$. The dilution rate is expected to revert to that of the steady jet once the puffs start to interact. A similar behavior is expected for the jets consisting of distinct vortex rings, except for the fluid forming the vortex cores. The latter would get mixed at a much slower pace.

VI. Summary

Scaling arguments, based on the motion of individual vortex ring and puffs in quiescent media, are developed for the penetration and mixing of pulsed jets in crossflow. The maximum penetration of pulsed jets arises when the jet consists of individual, thin-cored vortex rings. The penetration of pulsed jets made of noninteracting vortex rings and puffs scales with the fourth root of the velocity ratio, stroke ratio, and the axial distance. The penetration of a steady jet, on the other hand, scales with the axial distance to a power of $\approx$0.27–0.33 and the velocity ratio to a power of $\approx$0.7. The decay of mean concentration in such pulsed jets scales with the velocity ratio and distance to the $-3/4$th power. This indicates a more rapid dilution and mixing in comparison to that in the far field of a steady jet in crossflow.

A map has been developed to demarcate the various regimes of pulsed jets depending on the stroke ratio of the injected slug during each pulsing period and the duty cycle. Although this map is strictly valid for the fully modulated pulsed jets, it should also be applicable to acoustically and partially modulated jets in crossflow as long as the unsteady component of the jet velocity is significantly larger than the baseline. To verify the proposed scaling and refine the proportionality constants, experiments should be conducted with attention focused on systematic variation of pulsing parameters discussed in this paper.

It is important to note that both deep penetration into the crossflow and adequate dilution and mixing can be achieved with pulsed jets if the pulsing parameters are chosen specifically to create compact vortex rings for rapid penetration initially, and subsequent interaction among vortical structures within the desired axial distance to attain the needed dilution and mixing.

References

[1] Margason, R. J., "Fifty Years of Jet in Crossflow Research," Computational and Experimental Assessment of Jets in Cross Flow, AGARD CP-534, Winchester, U.K., 1993, pp. 1-1–1-41.

[2] Fearn, R., and Weston, R. P., "Vorticity Associated with a Jet in a Cross Flow," *AIAA Journal*, Vol. 12, No. 12, 1974, pp. 1666–1671.

[3] Broadwell, J. E., and Breidenthal, R. E., "Structure and Mixing of a Transverse Jet in Incompressible Flow," *Journal of Fluid Mechanics*, Vol. 148, Nov. 1984, pp. 405–412.

[4] Fric, T. F., and Roshko, A., "Vortical Structure in the Wake of a Transverse Jet," *Journal of Fluid Mechanics*, Vol. 279, Nov. 1994, pp. 1–47.

[5] Smith, S. H., and Mungal, M. G., "Mixing, Structure and Scaling of the Jet in Crossflow," *Journal of Fluid Mechanics*, Vol. 357, Feb. 1998, pp. 83–212.

[6] Hasselbrink, E. F., Jr., and Mungal, M. G., "Transverse Jet and Jet Flames. Part 1. Scaling Laws for Strong Transverse Jets," *Journal of Fluid Mechanics*, Vol. 443, Sept. 2001, pp. 1–25.

[7] Pratte, B. D., and Baines, W. D., "Profiles of the Round Turbulent Jet in a Cross Flow," *Journal of the Hydraulics Division ASCE*, Vol. 92, Nov. 1967, pp. 53–64.

[8] Johari, H., Pacheco-Tougas, M., and Hermanson, J. C., "Penetration and Mixing of Fully-Modulated Turbulent Jets in Crossflow," *AIAA Journal*, Vol. 37, No. 7, 1999, pp. 842–850.

[9] Keffer, J. F., and Baines, W. D., "The Round Turbulent Jet in a Cross-Wind," *Journal of Fluid Mechanics*, Vol. 15, No. 4, 1963, pp. 481–496.

[10] Kamotani, Y., and Greber, I., "Experiments on a Turbulent Jet in a Cross Flow," *AIAA Journal*, Vol. 10, No. 11, 1972, pp. 1425–1429.

[11] Karagozian, A. R., "An Analytical Model for the Vorticity Associated with a Transverse Jet," *AIAA Journal*, Vol. 24, No. 3, 1986, pp. 429–436.

[12] Muppidi, S., and Mahesh, K., "Study of Trajectories of Jets in Crossflow Using Direct Numerical Simulations," *Journal of Fluid Mechanics*, Vol. 530, May 2005, pp. 81–100.

[13] Crow, S. C., and Champagne, F. H., "Orderly Structure in Jet Turbulence," *Journal of Fluid Mechanics*, Vol. 48, No. 3, 1971, pp. 547–591.

[14] Vermeulen, P. J., Ramesh, V., and Yu, W. K., "Measurements of Entrainment by Acoustically Pulsed Axisymmetric Air Jets," *Journal of Engineering for Gas Turbines and Power*, Vol. 108, July 1986, pp. 479–484.

[15] Bremhorst, K., and Hollis, P. G., "Velocity Field of an Axisymmetric Pulsed, Subsonic Air Jet," *AIAA Journal*, Vol. 28, No. 12, 1990, pp. 2043–2049.

[16] Krueger, P. S., and Gharib, M., "Thrust Augmentation and Vortex Ring Evolution in a Fully Pulsed jet," *AIAA Journal*, Vol. 43, No. 4, 2005, pp. 792–801.

[17] Kelso, R. M., Lim, T. T., and Perry, A. E., "An Experimental Study of Round Jets in Cross-Flow," *Journal of Fluid Mechanics*, Vol. 306, Jan. 1996, pp. 111–144.

[18] Vermeulen, P. J., Chin, C., and Yu, W. K., "Mixing of an Acoustically Pulsed Air Jet with a Confined Crossflow," *Journal of Propulsion and Power*, Vol. 6, No. 6, 1990, pp. 777–783.

[19] Wu, J. M., Vakili, A. D., and Yu, F. M., "Investigation of the Interacting Flow of Nonsymmetric Jets in Crossflow," *AIAA Journal*, Vol. 26, No. 8, 1988, pp. 940–947.

[20] Eroglu, A., and Breidenthal, R. E., "Structure, Penetration, and Mixing of Pulsed Jets in Crossflow," *AIAA Journal*, Vol. 39, No. 3, 2001, pp. 417–423.

[21] Chang, Y. K., and Vakili, A. D., "Dynamics of Vortex Rings in Crossflow," *Physics of Fluids*, Vol. 7, No. 7, 1995, pp. 1583–1597.

[22] McCloskey, R. T., King, J. M., Cortelezzi, L., and Karagozian, A. R., "The Actively Controlled Jet in Crossflow," *Journal of Fluid Mechanics*, Vol. 452, Feb. 2002, pp. 325–335.

[23] Gordon, M., Cater, J. E., and Soria, J., "Investigation of the Mean Passive Scalar Field in Zero-Net-Mass-Flux Jets in Cross-Flow Using Planar-Laser-Induced Fluorescence," *Physics of Fluids*, Vol. 16, No. 3, 2004, pp. 794–808.

[24] Richards, J. M., "Puff Motions in Unstratified Surroundings," *Journal of Fluid Mechanics*, Vol. 21, Jan. 1965, pp. 97–106.

[25] Johari, H., Zhang, Q., Rose, M., and Bourque, S., "Impulsively Started Turbulent Jets," *AIAA Journal*, Vol. 35, No. 4, 1997, pp. 657–662.

[26] Gharib, M., Rambod, E., and Shariff, K., "A Universal Time Scale for Vortex Ring Formation," *Journal of Fluid Mechanics*, Vol. 360, April 1998, pp. 121–140.

[27] Hermanson, J. C., Wahba, A., and Johari, H., "Duty-Cycle Effects on Penetration of Fully Modulated, Turbulent Jets in a Crossflow," *AIAA Journal*, Vol. 36, No. 10, 1998, pp. 1935–1937.

[28] Rosenfeld, M., Rambod, E., and Gharib, M., "Circulation and Formation Number of Laminar Vortex Rings," *Journal of Fluid Mechanics*, Vol. 376, Dec. 1998, pp. 297–318.

[29] Glezer, A., and Coles, D., "An Experimental Study of a Turbulent Vortex Ring," *Journal of Fluid Mechanics*, Vol. 211, Feb. 1990, pp. 243–283.

[30] Grigg, H. R., and Stewart, R. W., "Turbulent Diffusion in a Stratified Fluid," *Journal of Fluid Mechanics*, Vol. 15, Feb. 1963, pp. 174–186.

[31] Diez, F. J., Bernal, L. P., and Faeth, G. M., "Round Turbulent Thermals, Puffs, Starting Plumes and Starting Jets in Uniform Crossflow," *Journal of Heat Transfer*, Vol. 125, Dec. 2003, pp. 1046–1057.

[32] Glezer, A., "The Formation of Vortex Rings," *Physics of Fluids*, Vol. 31, No. 12, 1988, pp. 3532–3542.

G. Candler
Associate Editor